REPORT DOCUMENTATION PAGE

Form Approved
OMB No. 0704-0188

1. AGENCY USE ONLY (Leave blank)	2. REPORT DATE	3. REPORT TYPE AND DATES COVERED
	18 March 1996	Technical

4. TITLE AND SUBTITLE

PATHWAYS TO NANOCRYSTALLINE III-V (13-15) COMPOUND SEMICONDUCTORS

5. FUNDING NUMBERS

N00014-95-1-0194
R&T Project 3135008---16

Dr. Harold E. Guard

6. AUTHOR(S)

R. L. Wells and W. L. Gladfelter

7. PERFORMING ORGANIZATION NAME(S) AND ADDRESS(ES)

Department of Chemistry
Duke University
Durham, NC 27708-0346

8. PERFORMING ORGANIZATION REPORT NUMBER

Technical Report
No. DU/DC/TR-65

9. SPONSORING / MONITORING AGENCY NAME(S) AND ADDRESS(ES)

Office of Naval Research
300 North Quincy Street
Arlington, VA 22217-5000

10. SPONSORING / MONITORING AGENCY REPORT NUMBER

11. SUPPLEMENTARY NOTES

Accepted for publication in the *Journal of Cluster Science*

12a. DISTRIBUTION / AVAILABILITY STATEMENT

Approved for Public Release
Distribution Unlimited

12b. DISTRIBUTION CODE

13. ABSTRACT *(Maximum 200 words)*

Discussed in this review are various solution-phase methodologies and specific chemical reactions involving molecular precursors and/or species derived therefrom which have been utilized to synthesize various binary and ternary nanocrystalline III-V (13-15) compound semiconductors.

14. SUBJECT TERMS	15. NUMBER OF PAGES
nanocrystalline, quantum dots, III-V (13-15) compound semiconductors, synthesis	36
	16. PRICE CODE

17. SECURITY CLASSIFICATION OF REPORT	18. SECURITY CLASSIFICATION OF THIS PAGE	19. SECURITY CLASSIFICATION OF ABSTRACT	20. LIMITATION OF ABSTRACT
Unclassified	Unclassified	Unclassified	Unlimited

OFFICE OF NAVAL RESEARCH

Grant N00014-95-1-0194
R&T Project 3135008---16

Dr. Harold E. Guard

Technical Report No. DU/DC/TR-65

Pathways to Nanocrystalline III-V (13-15) Compound Semiconductors

Richard L. Wells[1] and Wayne. L. Gladfelter[2]

1. Department of Chemistry, Duke University, Durham, NC 27708
2. Department of Chemistry, University of Minnesota, Minneapolis, MN 55455

Accepted for Publication in the *Journal of Cluster Science*

Duke University
Department of Chemistry,
P. M. Gross Chemical Laboratory
Box 90346
Durham, NC 27708-0346

18 March 1997

[JOURNAL OF CLUSTER SCIENCE: FRONTIERS IN CLUSTER SCIENCE SPECIAL ISSUE, 1997]

PATHWAYS TO NANOCRYSTALLINE III-V (13-15) COMPOUND SEMICONDUCTORS

Richard L. Wells†* and Wayne L. Gladfelter§

†*Department of Chemistry, P. M. Gross Chemical Laboratory, Duke University, Durham, NC 27708 (U.S.A.)*

§*Department of Chemistry, Smith Hall, University of Minnesota, Minneapolis, MN 55455 (U.S.A.)*

(Received ....., 1996)

CONTENTS

Abstract *- Discussed in this review are various solution-phase methodologies and specific chemical reactions involving molecular precursors and/or species derived therefrom which have been utilized to synthesize various binary and ternary nanocrystalline III-V (13-15) compound semiconductors.*

Keywords *- nanocrystalline, quantum dot, III-V (13-15) compound semiconductors, syntheses*

Introduction

The discovery of markedly different properties from the bulk materials and the promise of exploiting these properties for making devices has led to widespread research activity in the field of nanocrystalline materials, both on scientific and technological grounds [1]. For example, the theoretical prediction [2, 3] that semiconductor band gaps should increase as the dimensions of the material grow smaller has been investigated in luminescence [4, 5] and other spectroscopic studies [1, 5, 6]. This phenomenon is one example of the group of properties called quantum confinement effects, and materials which are constrained to the nanometer scale in all three dimensions (i.e., nanocrystals) are referred to as quantum dots (QD's) or Q-particles. Other characteristics predicted for nanoscopic semiconductors include diminished bulk recombination rates relative to films due to a lack of grain boundaries [7], unusually high nonlinear optical susceptibilities [5a], and depression in the melting temperature [8]. The majority of the experimental work done on compound semiconductor nanocrystals has focused on II-VI (12-16) materials such as CdS and CdSe

[9], because schemes for the facile synthesis and isolation of such III-V (13-15) particulates had not been forthcoming. In recent years, however, new and relatively facile synthetic routes yielding many of the possible binary, and even some ternary, III-V compound semiconductors in nanocrystalline form have been developed [10].

Designing synthetic schemes for the growth of nanocrystalline particles requires due consideration of the actual bond-forming steps (at the molecular level) and of the mechanism for controlling the size of the particles (at the microstructural level). Ultimately, more subtle control of the crystalline phase of a material will be desirable.

Presented in this review are various solution-phase methodologies and specific chemical reactions involving molecular precursors and/or species derived therefrom which have been utilized to synthesize these fascinating materials. Various terms are used herein to denote/describe the proportionate dimensions of the nanocrystalline materials. Domain size is the average diameter of particles estimated from powder X-ray diffraction (XRD) line broadening, thus making it the same as coherence length. Individual particle size is measured by transmission electron microscopy (TEM). The radius of curvature is a measure from the center to the surface of the particle without regard to crystallinity; therefore, it is the same as particle size.

Synthetic Methods

Dehalosilylation and Related Reactions

The use of dehalosilylation (or silyl halide elimination) between halogallanes and silylarsines, including tris(trimethylsilyl)arsine, $(Me_3Si)_3As$, to synthesize various gallium-arsenic compounds was

pioneered by Wells and coworkers [11], and we reported in 1989 that gallium arsenide, GaAs, could be prepared using this methodology (eq. 1) [12]. Alivisatos and coworkers reported in the following year that

$$GaCl_3 + (Me_3Si)_3As \xrightarrow{-3Me_3SiCl} GaAs \qquad (1)$$

GaAs nanocrystals (domain size 10 nm) were in fact produced by this reaction between $GaCl_3$ and $(Me_3Si)_3As$ as initially carried out in toluene at refluxing temperature in our laboratories [13] (Note: this and some subsequently discussed reactions which lead to nanocrystalline materials are summarized in Schemes 1-3). In addition, they demonstrated that the same reaction carried out in quinoline at reflux afforded somewhat smaller crystallites which were soluble in pyridine as well as in quinoline [13]. Thus, this was the first report of the synthesis of redissolvable GaAs nanocrystals which, on dissolution in quinoline, were said to be capped with solvent at the crystallite surface. Subsequently, Nozik and co-workers confirmed GaAs nanocrystals result from this reaction in quinoline; however, they argued that the crystallites were capped with such molecular species as polyquinoline and/or some quinoline complexes of gallium formed *in situ* [14]. Utilizing this same basic dehalosilylation reaction between $GaCl_3$ and $(Me_3Si)_3As$, but in a refluxing decane solution, Fitzmaurice and co-workers isolated GaAs nanocrystallites (3 nm average diameter) with no evidence of capping molecular species [15]. Additionally, they found that conducting the reaction in an autoclave at elevated pressure led to controlled growth of the crystallites. Interestingly, Nozik and co-workers demonstrated that colloidal GaAs nanocrystallites were produced by refluxing a triglyme (*i.e.*, triethylene

glycol dimethyl ether) solution of $Ga(acac)_3$ (acac = acetylacetonate) and $(Me_3Si)_3As$ [16]. In this modification of the dehalosilylation reaction, the acac ligands apparently affect the cleavage of the trimethylsilyl groups from the arsine, however, the fate of the acac ligands and trimethylsilyl groups were not reported.

In 1989, Wells and coworkers also reported that reaction of $InCl_3$ and $(Me_3Si)_3As$ afforded indium arsenide, however, the size of the crystallites and the effect of using other indium(III) halides on particle size were not detailed (eq. 2) [12]. A follow-up study revealed that reaction of toluene/ether solutions of $InCl_3$ and $(Me_3Si)_3As$ at room temperature produced a very fine brown-black powder. After annealing over the temperature range of 200-400 °C, the powder afforded InAs crystallites (zinc blende form) of up to 99.96% purity with an average domain size of approximately 9 nm (eq. 2) [17]. This is more than twice the average size

$$InX_3 + (Me_3Si)_3As \xrightarrow{-\ 3Me_3SiX} InAs \qquad (2)$$

X = Cl [11, 17]; X = Br, I [17]

of the 4 nm InAs particles reported by Uchida *et al.* from the reaction of $In(acac)_3$ with $As(SiMe_3)_3$ in triglyme at reflux (*i.e.*, 216 °C) [18]. InAs obtained from the 1:1 mole ratio reactions of $InBr_3$ and InI_3 with $(Me_3Si)_3As$ consisted of crystallites with average domain sizes of 10 and 12 nm, and purities of 99.65 and 85.95%, respectively.

In extending the dehalosilylation methodology, we have prepared dimeric compounds and adducts which were subsequently decomposed to yield nanocrystalline gallium phosphide, GaP (eqs. 3 and 4) [19, 20]. It is

$$GaX_3 + (Me_3Si)_3P \xrightarrow[))))]{-\ Me_3SiX} 1/2[X_2GaP(SiMe_3)_2]_2 \xrightarrow{-\ 2Me_3SiX} GaP \quad (3)$$

X = Cl [19,20], Br [20], I [20]

$$GaX_3 + (Me_3Si)_3P \xrightarrow{-\ 3Me_3SiX} X_3Ga{\bullet}P(SiMe_3)_3 \xrightarrow{} GaP \quad (4)$$

X = Cl, Br, I

of interest to note that reactions between the corresponding gallium(III) halides with $(Me_3Si)_3P$ in hydrocarbon solvents under prolonged sonication led to the isolation of the dimeric elimination-condensation products $[X_2GaP(SiMe_3)_2]_2$ (X = Cl, Br, I) (eq. 3). On the other hand, the individual adducts, $X_3Ga{\bullet}P(SiMe_3)_3$ [X = Cl, Br, I] were obtained in high yields from the same reaction mixtures at ambient temperatures in the absence of sonication (eq. 4). Upon heating to 320 °C, the bromo and iodo dimeric species, which were initially white crystalline materials, became yellow, then orange, and final annealing at 400-500 °C produced dark brown powders. The chloro-containing dimer was decomposed in a similar manner, but was not annealed. The (111), (220), and (330) zinc blende peaks of GaP were clearly evident in the XRD powder patterns of each of the resultant air-stable brown powders. The breadth of the peaks indicated the powders contained nanocrystalline particles, and application of the Scherrer formula established an average domain size of ca. 3 nm for the bromo and iodo compounds and ca. 1 nm for the chloro compound. Elemental analyses of the brown powders indicated a relatively large amount of impurity, as well as an excess of phosphorus. In a later study, Micic and co-workers synthesized colloidal dispersions of GaP QD's utilizing the reaction illustrated in equation 3 [21]. They found that heating a trioctylphosphine/trioctylphosphine oxide (TOP/TOPO) solution of $GaCl_3$

and $(Me_3Si)_3P$ to 270-320 °C gave amorphous GaP which could be converted to crystalline material in TOPO at 360 °C. Treatment of the latter with methanol as a precipitating and washing agent afforded GaP QD's soluble in toluene. From the XRD powder patterns and transmission electron microscopy (TEM), the average particle diameter was estimated to be 2 to 3 nm. No elemental analyses were reported; however, based on features in the optical absorption spectra of the GaP QD's, they were thought to be of high quality. It was also noted by these workers that GaP QD's can be synthesized by substituting a chlorogallium oxalate complex for $GaCl_3$ in the reaction with $(Me_3Si)_3P$ [21]. The preparation of this complex is described, but it had not been completely characterized. Pyrolysis of all three of the adducts, $X_3Ga{\bullet}P(SiMe_3)_3$, at 450 °C under vacuum resulted mainly in nanocrystalline cubic GaP with 4-5 nm average particle sizes as determined by XRD powder patterns and, for pyrolysis of the bromine adduct, by TEM. In addition, as shown from elemental analysis, small quantities of amorphous Si/C/H containing phases were also formed.

The initial use of dehalosilylation to prepare indium phosphide (InP) was by Barron and co-workers in 1989 [22]. They reported the 1:1 mole ratio reactions of InX_3 (X = Cl, Br, I) with $(Me_3Si)_3P$ to form oligomeric precursors $[X_2InP(SiMe_3)_2]_n$ with concomitant elimination of Me_3SiX. Thermolyses of these precursors under vacuum at 400-500 °C yielded "polycrystalline" InP; however, no mention was made of the size of the InP crystals. A further investigation of these reactions in our laboratory revealed the separate 1:1 mole ratio reactions of $InCl_3$ and $InBr_3$ with $(Me_3Si)_3P$ at room temperature in toluene/ether produced orange and yellow-orange oligomeric powders, respectively, (eq. 5) [17] similar to

those reported by Barron [22]. Thermolyses of these powders under vacuum over the range of 200-400 °C afforded nanocrystalline InP particles (eq. 5) with respective purities and In:P ratios of 91.53% and 1.00:1.09, and 93.08% and 1.00:1.03 from elemental analysis, and an average domain size from XRD of approximately 4 nm in both cases [17]. On the other hand, the 1:1 mole ratio reaction of InI_3 with $(Me_3Si)_3P$ at room temperature in toluene/ether gave the Lewis acid-base adduct $I_3In{\bullet}P(SiMe_3)_3$ (eq. 6) [17]. Bulk thermolysis of this adduct under vacuum over the range of 200-400 °C afforded nanocrystalline InP (eq. 6) of 84.06% purity, from elemental analysis, with an approximate average domain size of 2.5 nm, as shown by XRD, TEM, and UV/vis spectroscopy.

$$InX_3 + (Me_3Si)_3P \xrightarrow{-\ Me_3SiX} 1/n[X_2InP(SiMe_3)_2]_n \xrightarrow{-\ 2Me_3SiX} InP \quad (5)$$

X = Cl, Br

$$InI_3 + (Me_3Si)_3P \longrightarrow I_3In{\bullet}P(SiMe_3)_3 \xrightarrow{-\ 3Me_3SiI} InP \quad (6)$$

Alivisatos and co-workers recently utilized the reaction of $InCl_3$ and $(Me_3Si)_3P$ in TOPO at 265 °C to synthesize highly crystalline InP nanocrystals with diameters of 2-5 nm which can be subsequently capped with various species at 100 °C (eq. 7) [23]. These quantum-confined

$$InCl_3 + TOPO \longrightarrow InCl_3\text{-TOPO complex} \xrightarrow{+\ (Me_3Si)_3P}$$

$$InP\ (TOPO\ capped) \xrightarrow{+\ S\ (S = RNH_2,\ RSH,\ RPH_2)} InP\ (S\ and\ TOPO\ capped) \quad (7)$$

nanocrystals were monodisperse and soluble in various organic solvents. Based on XPS scans, it was noted that the In:P ratio varied from 0.74 to

0.97 with an average of 0.86 ± 0.07; however, after taking into account the contribution of the oxide layer to the signal, it was concluded that the ratio is nearly 1:1. Furthermore, XPS found no Cl or Si (less than 1% Cl and Si from bulk elemental analysis), but it established a 30 to 100% surface coverage by TOPO. By using selective precipitation techniques, the nanocrystals were size-separated into the narrowest size distributions ever reported for III-V nanocrystals, as evidenced from TEM imaging and XRD spectra.

The preceding process was a modification of the first reported synthesis of highly crystalline, mondisperse, and soluble InP QD's which utilized a partially characterized chloroindium oxalate complex and $(Me_3Si)_3P$ [21, 24] as the starting materials. In this study, Micic et al. demonstrated that InP QD's (mean diameter 2.6 ± 0.7 nm, from TEM) were readily produced on heating (270 °C) a TOPO solution of the orange InP precursor which resulted from the combination of the chloroindium oxalate complex and $(Me_3Si)_3P$.

Notwithstanding the quite extensive activity in the past few years in the use of dehalosilylation to prepare nanocrystalline arsenic- and phosphorus- containing III-V materials, *vide supra*, it was only very recently that this methodology was applied to the preparation of nanocrystals of an antimony-containing III-V material, viz., gallium antimonide, GaSb (eq. 8) [25]. Upon mixing pentane solutions of $GaCl_3$ and

$$GaCl_3 + (Me_3Si)_3Sb \xrightarrow{-\ 3Me_3SiI} \text{red-brown powder} \longrightarrow GaSb \qquad (6)$$

$(Me_3Si)_3Sb$, an orange-red color developed immediately with formation of a dark precipitate which, after 12 hours at room temperature, was isolated

as a red-brown powder. Annealing this amorphous intermediate at 400 °C afforded a black powder containing GaSb. Based on full elemental analysis the Ga:Sb ratio was found to be 1:1.1. Interestingly, the Ga and Sb constituted 75% of the sample weight, while C, H, Cl and Si accounted for only a total of another *ca.* 6%. The XRD pattern of the black powder confirmed the presence of cubic GaSb, as well as some Sb, and the average particle size of the GaSb was calculated to be 12 nm. The range of crystallite sizes obtained from a HRTEM micrograph was in good agreement with the average size obtained from the XRD data. In the study by Schulz *et al.* [25b], the same reaction was carried out in toluene, but the resultant dark orange solution and brown precipitate obtained on combining the reactants was refluxed for 24 hours to yield a black precipitate. Subsequent heating at 400 °C for 30 minutes afforded GaSb contaminated with small amounts of H, C, Cl and Si, and having a Ga:Sb mole ratio of 1:1.16 by elemental analysis. Based on SEM and TEM analyses, the crystallite size of the GaSb was in the range of 10 to 40 nm.

Dehalosilylation reactions also have proven to be an effective pathway to ternary (one group III element and two different pnicogens) nanocrystalline III-V compound semiconductors. Thus, we found that sonication of a toluene solution of the dimers $[I_2GaE(SiMe_3)_2]_2$ (E = P [19b], As [26]) afforded the gallium-mixed-pnicogen ring compound $I_2\overline{GaAs(SiMe_3)_2Ga(I)_2P}(SiMe_3)_2$ in very low (*ca.* 6%) yield (eq. 9) [27]. However, it was demonstrated that this same ring compound could be prepared in quantitative yield by combining and sonicating two molar equivalents of GaI_3 with one molar equivalent each of $(Me_3Si)_3As$ and $(Me_3Si)_3P$ in toluene solution at room temperature (eq. 9). [27]. Full

$$[I_2GaAs(SiMe_3)_2]_2 + [I_2GaP(SiMe_3)_2]_2$$

$$\xrightarrow{))))}$$

$$I_2\overline{GaAs(SiMe_3)_2Ga(I)_2P}(SiMe_3)_2 \xrightarrow{-\ 4Me_3SiI} GaAs_xP_y \qquad (9)$$

$$\xrightarrow[-\ 2Me_3SiI]{))))}$$

$$2GaI_3 + (Me_3Si)_3As + (Me_3Si)_3P$$

characterization of this novel precursor was achieved by a single crystal X-ray diffraction study, multinuclear NMR (^1H, ^{13}C, ^{31}P) , electron impact mass spectrometry, and elemental analyses (C, H, As, Ga, I, P). TGA studies indicated the compound eliminated four molar equivalents of Me_3SiI, as required for decomposition to the Ga_2AsP core. Bulk thermolysis at 400 °C afforded a brown-black powder (stable when exposed to air) which was shown by powder XRD and elemental analyses (C, H, As, Cl, Ga, P) to be nanocrystalline (domain size *ca.* 1 nm) $GaAs_xP_y$, (x = 0.65 and y = 0.52) with significant contamination by C, H, and I. [10a, 27b]. The XRD pattern of this powder displayed the (111) peak between the expected values for GaAs and GaP which, by Vegard's Law [28], indicated the presence of a solid solution of $GaAs_xP_y$ in the sample. The brown powder resulting from the thermolysis at 450 °C for 12 hours of a sample of the cyclic precursor was shown to be $GaAs_xP_y$ of 2.4 nm particle size, with the three major peaks in the XRD powder pattern being readily identifiable [10a].

In an effort to synthesize the ternary indium arsenide phosphide, two molar equivalents of $InCl_3$ with a mixture of one molar equivalent each of $(Me_3Si)_3As$ and $(Me_3Si)_3P$ were allowed to react in solution to afford a brown powder with an In:As:P ratio of 3.71:1.85:1.00 [10]. Subsequent thermolysis of this sample at 400 °C gave a lustrous black powder with a In:As:P ratio of 2.38:1.89:1.00, corresponding to $InAs_xP_y$

(x = 0.79, y = 0.42). The XRD powder pattern of this sample also showed it to be nanocrystalline (domain size *ca.* 9 nm), with (111), (220), and (311) reflections located between those expected for InP and InAs, again indicative by Vegard's Law of the presence of a ternary semiconductor. A high-resolution TEM image of this sample showed lattice lines for several nanocrystalline $InAs_xP_y$ particles ranging in size from 6 to 15 nm.

Also, formation of the ternary mixed-metal semiconductor gallium indium phosphide was attempted by us in a similar one-pot synthesis. The reaction of a solution-phase mixture of one molar equivalent each of $GaCl_3$ and $InCl_3$ with one molar equivalent of $(Me_3Si)_3P$ resulted in a light yellow powder with a Ga:In:P ratio of 1.04:1.00:1.05 Thermolysis of this powder at 400 °C yielded a brown powder with a Ga:In:P ratio of 2.69:1.00:4.16, corresponding to Ga_xIn_yP (x = 0.65, y = 0.24), with significant C, H, Cl, and Si (by difference) contamination. An XRD pattern showed it to be nanocrystalline (domain size ca. 1 nm), with (111), (220), and (311) reflections located between those expected for GaP and InP [10a], again indicative by Vegard's Law of the presence of a ternary Ga_xIn_yP mixed-metal semiconductor in the powder sample.

Micic *et al.* also synthesized nanocrystals of gallium indium phosphide but, rather than the trichlorides of the metals, they used a reaction mixture consisting of a chlorogallium oxalate complex, a chloroindium oxalate complex and $(Me_3Si)_3P$ (1:1:2.6 mole ratio mixed at room temperature in toluene) [21]. Heating this mixture in TOPO and tris(2-diphenylphosphinoethyl)phosphine at 300 °C, followed by separation, purification with methanol, and partial dissolution in a solution of TOPO in toluene, afforded 2.5 nm $GaInP_2$ QD's. Heating this solid with a yellow flame and subsequent redissolution in a toluene solution of TOPO

gave larger (6.5 nm) more crystalline particles of $GaInP_2$, the XRD powder pattern of which showed lattice spacings approximately the average of those of GaP and InP.

Reactions involving a group III metal trihalide with a silylpnictine in a 2:1 mole ratio have also afforded novel precursors to nanocrystalline binary materials. Thus, the reaction of two mole equivalents of $GaCl_3$ with one mole equivalent of $(Me_3Si)_3E$ (E = As, or P) resulted in the formation of the isolable yellow substance of unknown structure having the empirical formula Ga_2ECl_3 (eq. 10) [29, 19b]. These powders undergo $GaCl_3$

$$2GaCl_3 + (Me_3Si)_3E \xrightarrow{-3Me_3SiCl} 1/n(Ga_2ECl_3)_n \xrightarrow{-GaCl_3} GaE \qquad (10)$$
$$E = As, P$$

elimination at temperatures >300 °C to produce nanocrystalline GaAs [30] or GaP [19b] with a domain size of approximately 3 nm (from XRD powder patterns). Having observed that either the arsine or the phosphine could be used to synthesize the respective binary precursor, a successful effort was made to prepare the analogous precursor {viz., $[Ga_2(As/P)Cl_3]_n$} to the ternary gallium arsenide phosphide, $GaAs_xP_y$ (eq11) [30]. Thermolysis of

$$2GaCl_3 + 1/2(Me_3Si)_3As + 1/2(Me_3Si)_3P \xrightarrow{-3Me_3SiCl}$$

$$1/n[Ga_2(As/P)Cl_3]_n \xrightarrow{-GaCl_3} GaAs_xP_y \qquad (11)$$

the off-white $[Ga_2(As/P)Cl_3]_n$ at 400 °C resulted in elimination of $GaCl_3$ and subsequent formation of a dark brown powder. This powder was confirmed by XRD, XPS, and elemental analysis to be the ternary III-V compound semiconductor $GaAs_xP_y$ ($0.6 \leq x, y \leq 0.9$) [30]. From the XRD

powder pattern, it was determined that powder contained nanocrystals of the ternary having a domain size of *ca.* 3 nm. The reflections observed in this pattern were between those expected for GaAs and GaP, which would be expected according to Vegard's Law, which further confirmed the identity of this mixed-pnicogen compound semiconductor.

Alkali Metal Halide Elimination

The development in the Wells laboratories of a new, low temperature solution phase synthesis of nanocrystalline III-V semiconductors was reported in 1994 [31]. The reaction used is fundamentally similar to a general method described by Kaner and coworkers involving solid state metathesis (SSM) to synthesize binary III-V semiconductors by reacting sodium pnictides with Group III halides in autoclaved or sealed glass ampules at high temperatures [32]. In the typical solution phase metathesis (SPM) experiment, a group III metal trihalide dissolved in a glyme solvent was allowed to react *in situ* with $(Na/K)_3E$ (E = P, As, Sb) synthesized from Na/K and E in an aromatic solvent. (eqs. 12, 13). Nanocrystallites with average particle size of 4-35 nm can be prepared,

$$3(Na/K) + E \text{ ---------> } (Na/K)_3E \quad (12)$$
E = P, As, Sb

$$MX_3 + (Na/K)_3E \text{ --------> } 3(Na/K)X + ME \quad (13)$$
M = Ga; X = Cl, I
M = In; X = Cl, Br, I

and each of the following have been obtained: GaP (11 nm), GaAs (10 nm), GaSb (35 nm), InP (4 nm), InAs (11 nm), and InSb (26 nm). The particle sizes depend on the group III halide, the solvent, concentration and chain length of the glyme solvents. When $GaCl_3$ was dissolved in various

solvents and subsequently allowed to react with $(Na/K)_3As$, synthesized *in situ* in refluxing toluene, different average size particles of GaAs were obtained: toluene (36 nm), dioxane (36 nm), monoglyme (17 nm), and diglyme (10 nm). The crystallites were characterized by XRD, TEM, XPS, UV/vis, and elemental analysis. For a typical GaAs sample which was annealed at 350 °C, the elemental analysis showed a slight excess of Ga (Ga:As ratio 5.1:4.0, whereas halogen-containing impurities, carbon and hydrogen were 0.01%, 2-5% and <0.01%, respectively. The blue-shifted UV/vis absorption spectra gave clear evidence of quantum confinement in these nanoparticles.

Considerable attention has been given to as-prepared GaAs nanocrystallites (*i.e.*, material obtained by simple refluxing the reaction mixture). Extraction of such nanocrystals with methanol resulted in surface derivatization of GaAs quantum dots [10a, 33]. The surface bound methanol facilitated the formation of colloidal suspensions of GaAs, and such suspensions were stable for more than eighteen months. These capped GaAs nanoclusters present in the colloidal suspension were characterized by XRD, NMR, HRTEM, XPS, FTIR PAS (photoacoustic spectroscopy), EA (elemental analysis) and UV/vis. The average crystallite size obtained by evaporating methanol from the colloid was 5 nm, and HRTEM of the solids from the grey colloid showed lattice planes due to 3-11 nm particles. Centrifugation of the grey colloid resulted in settling of larger crystallites, leaving a reddish-orange colloid. An HRTEM image of the solid in this colloid showed the presence of crystallites smaller than 2 nm.

In recent related studies, heterogeneous reactions between $GaBr_3$ and Li_3N in refluxing aromatic (*i.e.*, xylene, mesitylene) or aromatic/diglyme

solvents were shown to be a successful route to nanocrystalline GaN powders (***Caution***: *Upon mixing, solid $GaBr_3$ and solid Li_3N react spontaneously as a self-igniting, highly exothermic, and uncontrollable process.*) (eq. 14) [34] . The reactions in solvents yielded, after removal of

$$GaBr_3 + Li_3N \text{ ----------> } 3LiBr + GaN \qquad (14)$$

solvent and LiBr with ether, grey precursors that were converted to nanocrystalline GaN and Ga upon heating at 450 °C under vacuum; the purity of the final product being improved by additional pyrolysis at 500 °C under a flow of NH_3. Based on nitrogen combustion analysis, a GaN content of only 53% was obtained from the latter product, but this number may not be meaningful due to the problems often associated with materials such as this, especially metal nitrides. XPS spectroscopy could not confirm this GaN content, because the method was found to yield unreliable nitrogen estimations due to preferential nitrogen sputtering from such materials. The crystallinity of the final product was dependent on both the solvent medium used for metathesis and the pyrolysis temperature. The product from the reaction in xylene, heated at 500 °C under an NH_3 atmosphere had a particle size of 5 nm (from Scherrer estimation applied to XRD powder pattern peaks). As evidenced from UV/vis spectroscopy, colloidal methanol solutions of the product showed a quantum confinement effect associated with up to a 0.88 eV blue shift of the bulk absorption edge of GaN. Such a shift corresponded to GaN nanocrystallites with a 3 nm diameter. TEM microscopy provided very strong evidence for nanocrystalline GaN particles, both in the bulk solid and the solid obtained from the clear, settled colloidal methanol solution after removal of volatiles. For the bulk solid, the particles consisted of

polycrystalline domains below 10 nm, with a significant fraction in the 5-7 nm range. Smaller nanocrystallites, with diameters less than 5 nm and mostly in the 3 to 4 nm regime, were observed for the solid contained in the methanol solution.

Using the same basic metathesis reaction as illustrated in eq. 14, but under different conditions, Qian and co-workers found that reaction of $GaCl_3$ with Li_3N in benzene at 280 °C under pressure in an autoclave produced nanocrystalline GaN [35]. This "benzene-thermal" process produced a dark-gray precipitate that was freed of LiCl with ethanol washing, and dried in vacuum at 100 °C. The XRD powder pattern indicated that the material produced consisted of mostly GaN with a wurtzite (*i.e.*, hexagonal) structure, but with a small amount GaN with a rock-salt (*i.e.*, cubic) structure. TEM images revealed the average size of the GaN crystallites to be 32 nm.

Thermolysis and Thermolysis-Ammonolysis

Gonsalves *et al.* recently reported the preparation of nanocrystalline GaN and its subsequent dispersal in poly(methyl)methacrylate (PMMA). The GaN was produced by heating the amide $[Ga(NMe_2)_3]_2$ at 600 °C in an NH_3 flow (eq. 16) [36]. The as-prepared material was a powder consisting

$$1/n[Ga(NMe_2)_3]_2 + NH_3 \text{ ----------> } 3Me_2NH + GaN \qquad (16)$$

of *ca.* 5 nm particles agglomerated into larger (*ca.* 50 nm) particles (from HRTEM image) and chemical analysis showed them to be deficient in nitrogen (empirical formula $GaN_{0.86}$). An XRD powder pattern exhibited peaks that corresponded to lattice planes of face-centered cubic (i.e., zinc blende) GaN, and examination of the HRTEM image revealed the material was face-centered cubic with numerous stacking faults. Sonication in the

presence of methylmethacrylate and subsequent polymerization afforded 5.5 ± 2.6 nm size GaN particles dispersed in PMMA.

Using related chemistry, Janik and Wells have synthesized a new nanocrystalline GaN precursor; viz., the polymeric gallium imide $[Ga(NH)_{3/2}]_n$, from the reaction of $[Ga(NMe_2)_3]_2$ with either gaseous or liquid NH_3 (eq. 17) [37]. Pyrolysis of the imide at 450-500 °C under

$$1/2[Ga(NMe_2)_3]_2 + 3/2NH_3 \xrightarrow{-3Me_2NH} 1/n[Ga(NH)_{3/2}]_n \xrightarrow{-1/2NH_3} GaN \quad (17)$$

vacuum or NH_3 flow afforded gray-yellowish and yellow-grayish products, respectively. Both were shown by XRD to be, remarkably, the same mixture of cubic and hexagonal close-packed layers of GaN that was reported earlier by Gladfelter and coworkers [38] (*vide infra*). The relatively sharp XRD powder pattern obtained for the solid from the pyrolysis at 500 °C under NH_3 matched the pattern reported in the above reference. The TEM micrograph and the electron diffraction pattern for supported the presence of relatively large particles of cubic GaN. On the basis of the relative width of the XRD powder patterns and the TEM micrographs, this solid consisted of larger and less disordered GaN crystallites (average 7 nm) than the solid from the pyrolysis at 450 °C under vacuum (average 2 nm). Elemental analysis showed the Ga:N atomic ratios were very close to 1:1, consistent with the formation of stoichiometric GaN and only small quantities of retained carbon (e.g., 0.22%, pyrolysis under NH_3).

Risbud, Power and coworkers have demonstrated that thermolysis of $(Me_2GaNPh_2)_2$ contained in silica aerogel affords 10-40 nm diameter GaN nanoparticles immobilized in the pores of the aerogel matrix [39]. Samples

prepared by incorporating the dimeric precursor into meticulously dried aerogel in a dry box (argon atmosphere) were pyrolyzed at *ca.* 200 °C for *ca.* 6 hours under a flow of N_2 and then annealed at 600 °C for 12-24 hours under a flow of NH_3. Powder XRD data were consistent with hexagonal (*i.e.*, wurtzite) GaN and a mean crystallite size of *ca.* 20 nm and, from TEM micrographs, the mean particle size was found to be *ca.* 23 nm.

In yet another very recent report, it has been shown by Fischer *et al.* that nanocrystalline hexagonal GaN results from the solid-state pyrolysis of $[Ga(N_3)_3]_\infty$ (***Caution***: *Solvent-free* $[Ga(N_3)_3]_\infty$ *is explosive and detonates violently on rapid heating above 280-300 °C*) (eq. 18) [40]. To affect this

$$[Ga(N_3)_3]_\infty \text{ ----------> } 4N_2 + GaN \qquad (18)$$

transformation safely, the azide precursor first was slowly heated to 250 °C with this temperature being maintained for 8 hours under a flow of N_2. This thermolysis afforded polycrystalline GaN as an off-white to gray, non-explosive powder which, on annealing at 800 °C for 10 minutes, resulted in the hexagonal GaN, as indicated from the powder XRD pattern. From elemental analysis the Ga:N ratio was shown to be a 1:0.96. According to the authors, nanocrystals of ca. 5-10 nm size (from TEM micrographs) were obtained by controlling the pyrolysis conditions.

Dihydrogen Elimination

As indicated previously, the pool of isolable single-source precursors to III-V nanocrystallites includes simple Lewis acid-base adducts of the type $X_3M{\bullet}EY_3$ (*e.g.*, $Cl_3Ga{\bullet}P(SiMe_3)_3$) or their elimination-condensation products such as $[X_2MEY_2]_n$ (*e.g.*, $[Cl_2GaP(SiMe_3)_2]_2$). In some cases, thermal decomposition of these precursors resulted in relatively clean, quite complete elimination of the easily removable XY (e.g., Me_3SiCl) and

condensation of the ME solid network. The most desirable elimination-condensation reactions will yield the solid product at relatively low temperatures with complete removal of the XY moiety without itself being decomposed and incorporated into the solid state product. One obvious ideal leaving group is dihydrogen; however, compounds of the type $H_3M{\cdot}EH_3$ and $[H_2MEH_2]_n$ containing the heavier group III and group V elements are not readily accessible or stable. However, in 1990, Gladfelter and coworkers reported the synthesis of one such compound; *viz.*, $(H_2GaNH_2)_3$ [38a], and subsequently showed from the pyrolysis of white powdered samples that it is an excellent precursor to nanocrystalline GaN (eq. 18) [38b]. Decomposition with weight loss occurs primarily at 150 °C,

$$(H_2GaNH_2)_3 \text{ ---------> } 6H_2 + GaN \qquad (18)$$

as shown by TGA analysis, with the evolution of H_2 and some NH_3 which was verified by mass spectral analysis. Based on the weight of the residue remaining after heating to 500 °C and elemental analysis, the resultant dark gray to black powder had the empirical formula $GaN_{0.83}$. It was surmised that the excess gallium may be surface bound. At 180 ° C, the powder was XRD amorphous, but it became crystalline at 600 °C and consisted of ca. 6 nm particles, as evidenced from TEM and broadening of peaks in the XRD powder pattern. Somewhat surprisingly, this nanocrystalline GaN was found from modeling the XRD data to have a structure that is best described as a random arrangement of stacking planes with an equal amount of cubic and hexagonal planes. A topotactic relationship between the precursor $(H_2GaNH_2)_3$ and the final product was proposed to play a role in the formation of the kinetically favored cubic (zinc blende) GaN as compared with the nitride's thermodynamically stable

and common hexagonal (wurtzite) form.

Alcoholysis

As indicated in the previous section, one very important aspect of the use of single-source precursors to form desired nanocrystalline materials is the efficient and clean removal of the ligands bound to the central elements. A novel approach of affecting this removal was the alcoholysis of appropriate compounds; a methodology first reported by Theopold and coworkers (eq. 19) [41], then pursued in Buhro's laboratory [10b, 42].

$1/n[RR'ME(SiMe_3)_2]_n + 2R''OH \text{ ----> } RH + R'H + 2R''OSiMe_3 + ME$ (19)
R = R' = C_5Me_5, M= Ga, E = As, n = 1; R"= *t*-Bu [41a,b]
R = C_5Me_5, R' = Cl, M= In, E = P, n = 2; R"= Me [41a], *t*-Bu [41b]
R = R' = Me_3SiCH_2, M = In, E = P, n = 2; R" = Me [41c]
R = Me_3SiCH_2, R' = Cl, M = In, E = P, n = 2; R" = Me [41C]
R = R' = Me_3CCH_2, M = In, E = P, n = 2; R" = Me [41c]
R = R' = Me_3C, M = In, E = P, n = 2; R" = Me [10b, 42]

Reaction of the above arsinogallane (eq. 19) with *tert*-butyl alcohol effectively removed the Me_3Si and C_5Me_5 ligands to yield a reddish powder which was shown from an XRD powder pattern and SEM and elemental analyses to be amorphous GaAs. Annealing the powder at 500 °C gave crystalline bulk GaAs. On adding an excess of the alcohol to a THF solution of this compound, the yellow solution became orange and finally red-brown. A series of absorption spectra used to monitor the reaction revealed a continuous red shift of the absorption signal with time. Based on these observations, it was concluded that small clusters of GaAs (average particle size ca. 6 nm) were being formed during the initial stages of the reaction. Similarly, alcoholysis of the above first four phosphinoindane precursors (eq. 19) produced amorphous InP particles

which, upon heating, become crystalline.

On the other hand, methanolysis of $[(Me_3C)_2InP(SiMe_3)_2]_2$ in toluene at room temperature resulted in a yellow-orange solution after 10 hours which, on refluxing for 24 hours, afforded a black solid consisting primarily of polycrystalline InP and a small amount of In [42a]. Elemental analysis showed only a minimal amount of carbon (1.02%) and hydrogen (0.08%), and from the XRD powder pattern, the InP crystallites had an average coherence length of 11 nm. Decreasing the initial stirring time resulted in 9 to 16 nm lengths of InP, and 10-100 nm x 50-1000 nm crooked fibers were evident in TEM images. The reaction of $[(Me_3C)_2InP(SiMe_3)_2]_2$ with methanol proceeded through several fully characterized molecular intermediates and ultimately led to complete substitution of the trimethylsilyl groups with hydrogens. The cyclic trimer, $[(Me_3C)_2InPH_2]_3$, which was also formed directly by an alkane elimination reaction involving $(Me_3C)_3In$ and PH_3, underwent further proton-catalyzed isobutane elimination to produce $(InP)_n$ fragments. The reaction solutions also contained nanometer-sized droplets of In, apparently formed as a side product when the organoindium reagent included tertiary butyl ligands. These In droplets acted as a growth medium by dissolving the $(InP)_n$ fragments and promoting the formation of InP fibers. This crystal growth pathway was coined a SLS mechanism (solution-liquid-solid) [42a,b].

It is interesting to note here that conventional organometallic chemical vapor deposition (OMCVD) alkane elimination reactions have been utilized by others to prepare III-V clusters/nanocrystallites but, for the most part, the particulates are produced in the gas phase or are imbedded in a host material, such as Vycor glass [43], nanochannel glass [44] or zeolite Y [1b].

For example, using OMCVD methane elimination reactions between PH_3 or AsH_3 with either Me_3Ga or Me_3In, but with the metal alkyls in the porous glass, GaP, InP, GaAs and InAs clusters of 9 to 10 nm were formed inside the glass, as determined by XRD (eq. 20) [43b]. In one report, GaAs

$$Me_3M + EH_3 \text{ ----> } 3MeH + ME \qquad (20)$$

M = Ga or In

E = P or As

particles were prepared from Me_3Ga and AsH_3 in a vapor-phase epitaxy (OMVPE) reactor and they were shown to be highly faceted 10-20 nm single crystals, as evidenced from TEM micrographs [45]. Two other gas-phase approaches have been utilized to prepare GaAs arsenide clusters; namely, molecular beam epitaxy (MBE) to give 2.5 to 6 nm size particles (from TEM) which were deposited on silica [46], and explosive vaporization of bulk GaAs to yield 5 to 10 nm size clusters (from TEM of clusters collected on holey carbon) [47].

Size and Phase Control

The remarkable achievements in the preparation of II-VI semiconductor particles have allowed the production of particles with a controllable and narrow size distribution by performing the growth within surfactant micelles [48] or by separating the nucleation and growth steps [49]. In surfactant-controlled growth of CdSe particles within inverse micelles, the growing particle was protected by the surfactant, and subsequent steps that alter the particle size, such as Ostwald ripening, were prevented (or least significantly slowed) [48]. The surfactant also preventd the particles from agglomerating, and allowed redissolution following isolation. This method was a significant improvement of the

arrested-precipitation method.

The most impressive control of particle size achieved to date involves separating the nucleation and growth steps. The synthesis of nanocrystalline CdSe, for example, utilized organometallic precursors as the Cd^{2+} source (Me_2Cd) and either $Se(SiMe_3)_2$ or SeP(n-octyl)$_3$ as a convenient source of the Group 16 element [49]. The entire reaction was conducted in a high boiling solvent mixture comprised of P(n-octyl)$_3$ and OP(n-octyl)$_3$; both of which act to stabilize the surface of the particle by ligation. Nucleation and subsequent rapid quenching occurred by combining approximately equal volumes of solutions which contained the reagents; one at 230°C and the other at 25°C. The initial high temperature promoted particle nucleation; this step occurred to a limited extent as both the temperature and the degree of supersaturation dropped quickly. The growth continues at elevated temperatures, and this method utilized Ostwald ripening to sharpen the particle size distribution.

Although the above methods produced narrow particle size distributions, further separation was necessary to purify the ultimate product. Both size exclusion chromatographic procedures and selective precipitation have been employed to this end [48, 49].

From these successful studies several characteristic trends, especially relevant for the synthesis of II-VI semiconducting particles, are evident.

- If the native reactivity of the particle surface is high, the particles must be coated with a protective layer.
- This protective layer should enhance the solubility and limit the agglomeration of the particles.
- Formation of truly narrow size distributions requires a separation of the solubilized particles.

- The particle size distribution can be manipulated by kinetic (inverse micelle method) or thermodynamic (Ostwald ripening) considerations during the synthesis.

As can be seen from the results outlined in this review, direct application of the methods optimized for II-VI compounds to III-V semiconductors has met with limited success. In part, the higher lattice energies of the III-V's may require substantially higher temperatures for promoting phenomena such as Ostwald ripening. Secondly, the combined impact of the phosphine and phosphine oxide may be specific to the II-VI materials. Nanocrystalline InP particles were prepared by Alivasatos and coworkers via adaptation of the TOPO/TOP method [23], however, it was noted that both nucleation and growth occur simultaneously over the entire synthesis leading to a broad particle size distribution. Subsequent separation of the particles by fractional precipitation, however, did lead to the most monodisperse (20% standard deviation) distribution yet observed for III-V particles.

Variation of the solvent and other ligands appears to contribute to particle size control, although the underlying reasons for the observations remain obscure. In one report the size of nanocrystalline GaAs particles, prepared by the alkali-metal halide elimination, decreased measurably as the solvent was changed from dioxane (36 nm) to monoglyme (17 nm) to diglyme (10 nm) [10a, 31]. It was noted that glyme solvents tend to break up the known dimeric structures of the starting halides (*e. g.* $GaCl_3$) and form ionic coordination complexes. Such alteration of the starting material would impact the rates of subsequent chemical reactions involved in particle synthesis. The glyme solvents may have stabilized particles with a given radius of curvature, thus preventing or at least slowing subsequent

particle growth.

Virtually all of the III-V particles prepared to date had the same zinc-blende structure as the bulk material. The synthetic method, however, did seem to affect the structure of nanocrystalline GaN. As discussed nanocrystalline GaN prepared from $[H_2GaNH_2]_3$ and from $[Ga(NH)_{3/2}]_n$ exhibited an equal mix of cubic and hexagonal layers in a random arrangement. In addition, a rock salt phase of nanocrystalline GaN was reported in the reaction of Li_3N with $GaCl_3$ in benzene at 280 °C. Under equilibrium conditions, this high pressure phase of GaN does not form below 37 GPa. These observations demonstrate the feasibility of using kinetic control to determine the phase of the nanocrystalline products. Much work is needed, however, to understand and control these reactions.

Concluding Remarks

As illustrated here, a number of reaction pathways leading to a significant variety of III-V nanocrystalline materials have been forthcoming in the relatively short time period beginning with 1989. In the specific case of GaN, it was only in 1995 that the first report was made, yet six new schemes have appeared in 1996. Undoubtedly, other methodologies and pathways for producing these novel and intriguing materials are in the offing. This preparative chemistry remains an important aspect of future studies, but perhaps the greater challenge that lies ahead is that of size-control and uniform surface passivation. Indeed, we look forward to helping meet these challenges, as we hope many others will do, and we anticipate the technological applications that we suspect are on the horizon for III-V nanocrystal/quantum dots.

Acknowledgments

The authors gratefully acknowledge the organizations who have provided financial support for our work discussed in this review: Office of Naval Research, Air Force Office of Scientific Research, Lord Foundation of North Carolina, Duke University Research Council (RLW); National Science Foundation, NSF Center for Interfacial Engineering, Minnesota Supercomputer Institute (WLG). In addition, we thank our many co-workers for their many fine contributions to our research in this area (see references for their names). Finally, RLW wishes to thank the Department of Chemistry, University of Minnesota at Minneapolis for allowing him to be in residence during his sabbatical leave and the writing of this review.

References

1. See, for example, the following and references cited therein: (a) A. Henglein (1989). *Chem. Rev.* **89**, 1861. (b) G. D. Stucky and J. E. MacDougall (1990). *Science* **247**, 669. (c) L. E. Brus, and M. L. Steigerwald (1990). *Accts. Chem. Res.* **23**, 183. (d) G. D. Stucky (1992). *Prog. Inorg. Chem.* **40**, 99. (e) H. Weller (1993). *Adv. Mater.* **5**, 88. (f) R. W. Siegel (1993). *Physics Today* **46**, 64. (g) M. A. Reed (1993). *Science* **262**, 195. (h) M. A. Reed (1993). *Sci. Am.* **268**, 118. (i) Special Issue (1993). Isr. J. Chem. 33(1). (j) A. P. Alivisatos (1995). *MRS Bulletin* **20**, 23. (k) A. P. Alivisatos (1996). *Science* **271**, 933. (l) A. P. Alivisatos (1996). J. Phys. Chem. **100**, 13226

2. L. E. Brus (1984). *J. Chem. Phys.* **80**, 4403.

3. M. V. Rama Krishna and R. A. Friesner (1991). *J. Chem. Phys.* **95**, 8309.

4. M. Grundmann, J. Christen, N. N. Ledentsov, J. Böhrer, D. Bimberg, S. S. Ruvimov, P. Werner, U. Richter, U. Gösele, J. Heydenreich, V. M. Ustinov, A. Yu Egorov, A. E. Zhukov, P. S. Kop'ev, and Zh. I Alferov (1995). *Phys. Rev. Lett.* **74**, 4043.

5. (a) Y. Wang (1991). *Accts. Chem. Res.* **24**, 133. (b) K. Kash (1990). *J. Luminescence* **46**, 69-82.

6. R. J. D. Miller, G. L. McLendon, A. J. Nozik, W. Schmickler, and F. Willig, *Surface Electron Transfer Processes* (VCH Publishers, New York, 1995) Chapter 6 and references therein.

7. G. J. Meyer and P. C. Searson (1993). *Electrochem. Soc. Interface* **2**, 23.

8. (*a*) A. N. Goldstein, C. M. Echer, and A. P. Alivisatos (1992). *Science* **256**, 1425. (*b*) A. P. Alivisatos and A. N. Goldstein (1993). *U.S. Patent No.* **5,262,357**.

9. (*a*) C.-H. Fischer and A. Henglein (1989). *J. Phys. Chem.* **93**, 5578. (*b*) V. L. Colvin, A. N. Goldstein, and A. P. Alivisatos, (1992). *J. Am. Chem. Soc.* **114**, 5221. (*c*) B. Zorman, M. V. Ramakrishna, and R. A. Friesner (1995). *J. Phys. Chem.* **99**, 7649. (*d*) H. Noglik and W. Pietro (1995). *Chem. Mater.* **7**, 1333. (*e*) R. A. Hobson, P. Mulvaney, and F. Grieser (1994). *J. Chem. Soc., Chem. Commun.* 823.

10. (a) L. I. Halaoui. S. S. Kher, M. S. Lube, S. R. Aubuchon, C. R. S. Hagan, R. L. Wells, L. A. Coury, Jr., *in* G.-M. Chow and K. E. Gonsalves (eds.), *ACS Symposium Ser. 622, Nanotechnology: Molecularly Designed Materials* (American Chemical Society, Washington, DC 10b1996), pp 178-194. (b) W. E. Buhro (1994). *Polyhedron* **13**, 1131.

11. (a) C. G. Pitt, A. P. Purdy, K. T. Higa, and R. L. Wells (1986). *Organometallics* **5**, 1266. (b) R. L. Wells (1992). *Coord. Chem. Rev.* **112**, 273.

12. (a) R. L. Wells, C. G. Pitt, A. T. McPhail, A. P. Purdy, S. Shafieezad, and R.B. Hallock (1989). *Chem. Mater.* **1**, 4. (b) R. L. Wells, C. G. Pitt, A. T. McPhail, A. P. Purdy, S. Shafieezad, and R. B. Hallock (1989). *Mater. Res. Soc. Symp. Proc.* **131**, 45.

13. M. A. Olshavsky, A. N. Goldstein, and A. P. Alivisatos (1990). *J. Am. Chem. Soc.* **112**, 9438.

14. H. Uchida, C. J. Curtis, and A. J. Nozik (1991). *J. Phys. Chem.* **95**, 5382.

15. L. Butler, G. Redmond, and D. Fitzmaurice (1993). *J. Phys. Chem.* 97, 10750.

16. H. Uchida, C. J. Curtis, P. V. Kamat, K. M. Jones, and A. J. Nozik (1992). *J. Phys. Chem.* **96**, 1156.

17. R. L. Wells, S. R. Aubuchon, S. S. Kher, M. S. Lube, and P. S. White (1995). *Chem. Mater.* **7**, 793

18. H. Uchida, T. Matsunaga, H. Yoneyama, T. Sakata, H. Mori, T. Sasaki (1993). *Chem. Mater.* **5**, 716.

19. (a) R. L. Wells, M. F. Self, A. T. McPhail, S. R. Aubuchon, R. C. Woudenberg, and J. P. Jasinski (1993). *Organometallics* **12**, 2832. (b) S. R. Aubuchon, A. T. McPhail, R. L. Wells, J. A. Giambra, and J. R. Bowser (1994). *Chem. Mater.* **6**, 82.

20. J. F. Janik, R. A. Baldwin, R. L. Wells , W. T. Pennington, G. L. Schimek, A. L. Rheingold, and L. M. Liable-Sands (1996). *Organometallics* **15**, 5385.

21. O. I. Micic, J. R. Sprague, C. J. Curtis, K. M. Jonesm, J. L. Machol, A. J. Nozik, H. Giessen. B. Fluegel, G. Mohs, and N. Peyghambarian (1995). *J. Phys. Chem.* **99**, 7754.

22. (a) M. D. Healy, P. E. Laibinis, P. D. Stupik, and A. R. Barron (1989). *Mat. Res. Soc. Symp. Proc.* **131**, 83. (b) M. D. Healy, P. E. Laibinis, P. D. Stupik, and A. R. Barron (1989). *J. Chem. Soc. Chem. Commun.* 359.

23. A. A. Guzelian, J. E. B. Katari, A. V. Kadavanich, U. Banin, K. Hamad, E. Juban, A. P. Alivisatos, R. H. Wolters, C. C. Arnold, and J. R. Heath (1996). *J. Phys. Chem.* **100**, 7212.

24. O. I. Micic, C. J. Curtis, K. M. Jones, J. R. Sprague, and A. J. Nozik (1994). *J. Phys. Chem.* **98**, 4966.

25. (a) R. A. Baldwin, E. E. Foos, R. L. Wells, G. P. A. Yap, and A. L. Rheingold (1996). *Abstracts of Papers, 211th American Chemical Society National Meeting* (New Orleans, LA, March 24-29, 1996) INOR 198. (b) S. Schulz, L. Martinez, and J. L. Ross (1996). *Adv. Mater. Opt. Electron.* **6**, 185. (c) R. A. Baldwin, E. E. Foos, and R. L. Wells (1997). *Mater. Res. Bulletin* **32**, 15.

26. J. D. Johansen, A. T. McPhail, and R. L. Wells (1992). *Adv. Mater. Opt. Electron.* **1**, 29.

27. R. L. Wells, A. T. McPhail, P. S. White, M. S. Lube, and L. J. Jones III (1994). *Phosphorus, Sulfur, and Silicon* **93-94**, 329. (b) R. L. Wells, S. R. Aubuchon, M. S. Lube, P. S. White (1995). *Main Group Chemistry* **1**, 81.

28. (a) B. D. Cullity, *Elements of X-Ray Diffraction, 2nd edn.* (Addison-Wesley Reading, MA, 1978), pp 375-377. (b) J. B. Wiley, R. B. Kaner (1992). *Science* **255**, 1093.

29. R.L. Wells, R.B. Hallock, A. T. McPhail, C. G. Pitt, J. D. Johansen (1991). *Chem. Mater.* **3**, 381.

30. S. R. Aubuchon, M. S. Lube, R. L. Wells (1995). *Chem. Vap. Deposition* **1**, 28.

31. (a) S.S. Kher and R.L. Wells (1994). *Chem. Mater.* **6**, 2056. (b) S.S. Kher and R.L. Wells (1994). *Mater. Res. Soc. Symp. Proc.* **351**, 293. (c) S.S. Kher and R.L. Wells (1995). *U.S. Patent No.* **5,474,59**.

32. (a) R. E. Treece, G. S. Macala, L. Rao, D. Franke, H. Eckert, and R. B. Kaner (1993). *Inorg. Chem.* **32**, 2745. (b) R. E. Treece, E. G. Gillan, R. M. Jacubinas, J. B. Wiley, and R. B. Kaner (1992). *Mater. Res. Soc. Symp. Proc.* **271**, 169. (c) R. E. Treece, G. S. Macala, and R. B. Kaner (1992). *Chem. Mater.* **4**, 9. (d) D. Franke, H. Eckert, R. B. Kaner, and R. E. Treece (1993). *Anal. Chim. Acta* **283**, 987. (e) J. B. Wiley and R. B. Kaner (1992). *Science* **255**, 1093.

33. S.S. Kher and R.L. Wells (1996). *NanoStructured Materials* **7**, 591.

34. (a) J. F. Janik and R.L. Wells (1996). *Abstracts of Papers, 211th American Chemical Society National Meeting* (New Orleans, LA, March 24-29, 1996) INOR 196. (b) J. F. Janik and R.L. Wells (1996). *European J. Solid State and Inorg. Chem.* **33**, 1079.

35. Y. Xie, Y. Qian, W. Wang, S. Zhang, and Y. Zhang (1996). *Science* **272**, 1926.

36. K. E. Gonsalves, G. Carlson, S. P. Rangarajan, M. Bemaissa, and M. Jose-Yacaman (1996). *J. Mater. Chem.* **6**, 1451.

37. J. F. Janik and R.L. Wells (1996). *Chem. Mater.* **8**, 2708.

38. (a) J.-W. Hwang, S. A. Hansen, D. Britton, J. F. Evans, K. F. Jensen, and W. L. Gladfelter (1990). *Chem. Mater.* **7**, 517. (b) J.-W. Hwang, J. P. Campbell, J. Kozubowski, S. A. Hansen, J. F. Evans, and W. L. Gladfelter (1995). *Chem. Mater.* **7**, 517.

39. T. J. Goodwin, V. J. Leppert, C. A. Smith, S. H. Risbud, M. Niemeyer, P. P. Power, H. W. H. Lee, and L. W. Hrubesh (1996). *Appl. Phys. Lett.* **69**, 3230.

40. R. A. Fischer, A. Miehr, E. Herdtweck, M. R. Mattner, O. Ambacher, T. Metzger, E. Born, S. Weinkauf, C. R. Pulham, and S. Parsons (1996). *Chem. Eur. J.* **2**, 1353.

41. (a) E. K. Byrne, L. Parkanyi, and K. H. Theopold (1988). *Science* **241**, 332. (b) E. K. Byrne, T. Douglas, and K. H. Theopold (1989). *Mater. Res. Soc. Symp. Proc.* **131**, 59. (c) T. Douglas and K. H. Theopold (1991). *Inorg. Chem.* **30**, 594.

42. (a) W. E. Buhro (1996). *Personal communication.* (b) T. J. Trentler, K. M. Hickman, S C. Goel, A. M. Viano, P. C. Gibbons, and W. E. Buhro (1995). *Science* **270**, 1791.

43. (a) J.C. Luong, and N. F. Borrelli (1989). *Mater. Res. Soc. Symp. Proc.* **144**, 695. (b) Y. Wang and N. Herron (1991). *Res. Chem. Intermed.* **15**, 17. (c) B. L. Justus, R. J. Tonucci, and A. D. Berry (1992). *Appl. Phys. Lett.* **61**, 3151.

44. R. J. Tonucci, B. L. Justus, A. J, Campillo, and C. E. Ford (1992). *Science* **258**, 783.

45. P. C. Sercel, W. A. Saunders, H. A. Atwater, K. J. Vahala, and R. C. Flagan (1992). *Appl. Phys. Lett.* **61**, 696.

46. C. J. Sandroff, J. P Harbison, R. Ramesh, M. J. Andrejco, M. S. Hegde, D. M. Hwang, C. C. Chang, and E. M. Vogel (1989). *Science* **245**, 391.

47. W. A. Saunders, P. C. Sercel, H. A. Atwater, K. J. Vahala, and R. C. Flagan (1992). *Appl. Phys. Lett.* **60**, 950.

48. M. L. Steigerwald, A. P. Alivisatos, J. M. Gibson, T. D. Harris, R. Kortan, A. J. Muller, A. M. Thayer, T. M. Duncan. D. C. Douglass, and L. E. Brus (1988). *J. Am. Chem. Soc.* **110**, 3046.

49. C. B. Murray, D. J. Norris, and M. G. Bawendi (1993). *J. Am. Chem. Soc.* **115**, 8706.

Legends for Schemes

Scheme 1. Pathways to Nanocrystalline GaE (E = P, As).

Scheme 2 Pathways to Nanocrystalline InE (E = P, As).

Scheme 3 Pathways to Nanocrystalline GaN.

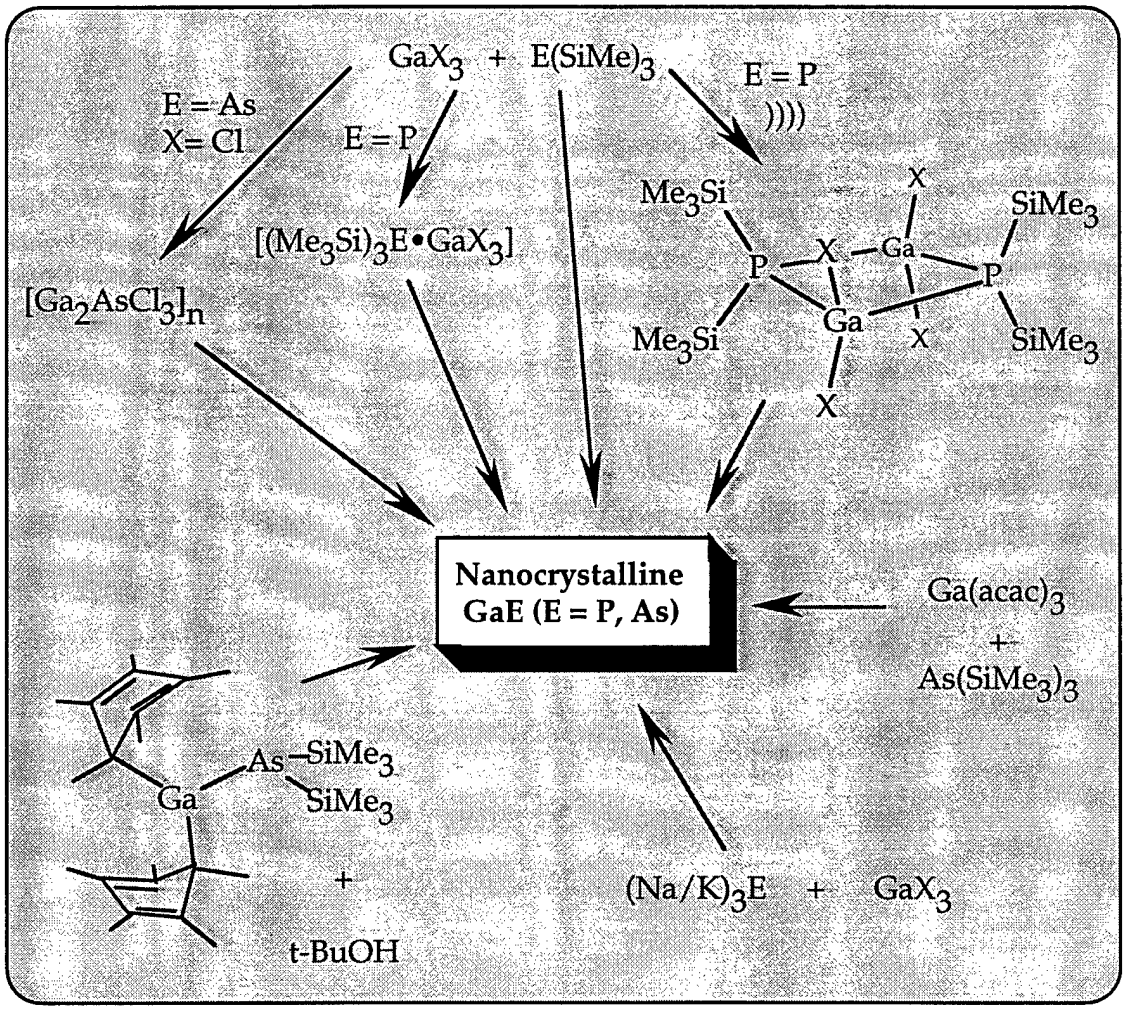
GaX3 + E(SiMe)3
E = As
X= Cl
E = P
E = P
[Ga2AsCl3]n
[(Me3Si)3E•GaX3]
Me3Si
X
SiMe3
P
X
Ga
P
Ga
Me3Si
X
SiMe3
X
Nanocrystalline
GaE (E = P, As)
Ga(acac)3
+
As(SiMe3)3
Ga
As–SiMe3
SiMe3
+
t-BuOH
(Na/K)3E + GaX3

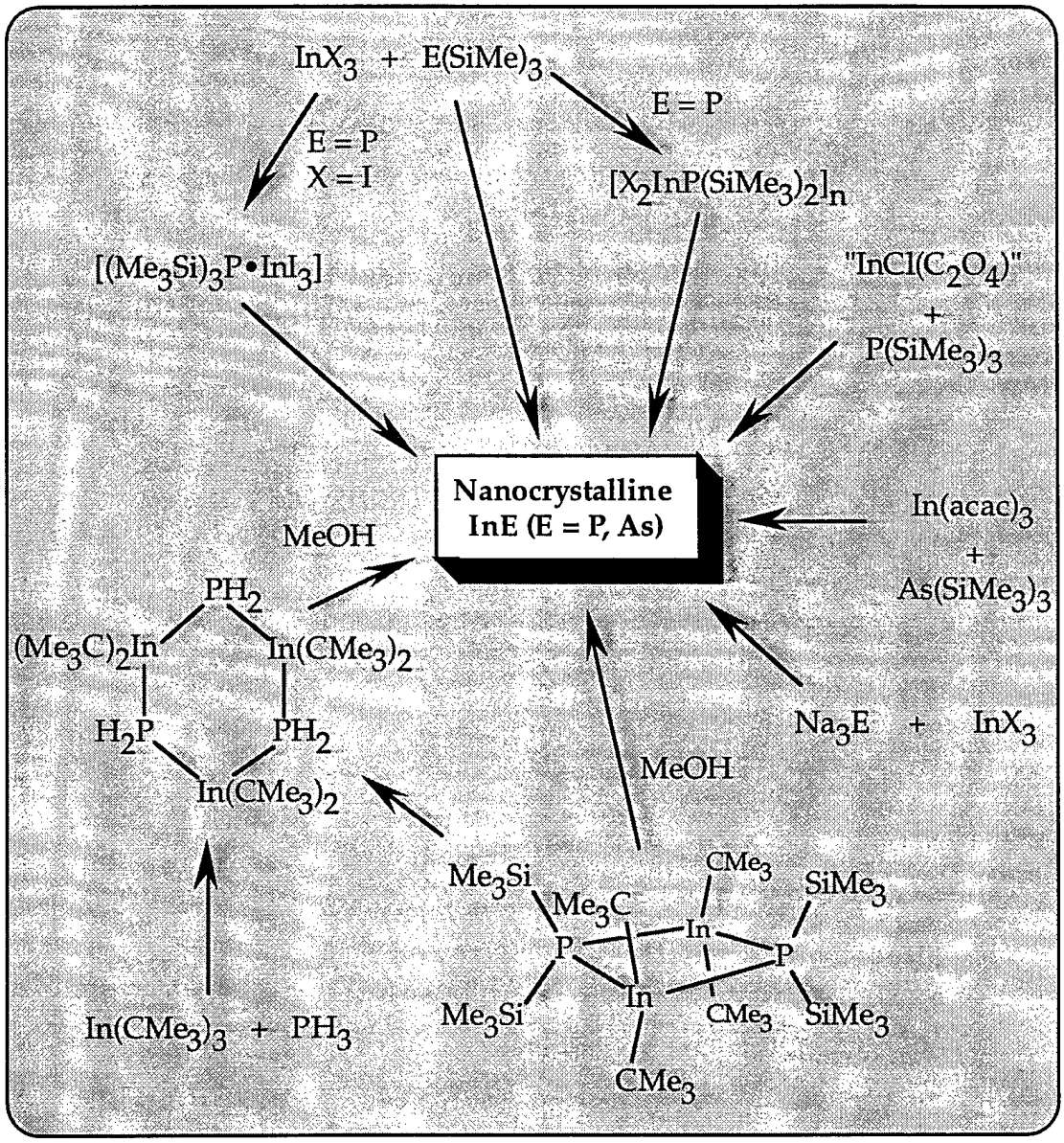
InX3 + E(SiMe)3
E = P
E = P
X = I
[X2InP(SiMe3)2]n
[(Me3Si)3P•InI3]
"InCl(C2O4)"
+
P(SiMe3)3
Nanocrystalline
InE (E = P, As)
In(acac)3
+
As(SiMe3)3
MeOH
PH2
(Me3C)2In
In(CMe3)2
H2P
PH2
In(CMe3)2
Na3E + InX3
MeOH
Me3Si
Me3C
CMe3
SiMe3
P
In
P
Me3Si
In
CMe3
SiMe3
CMe3
In(CMe3)3 + PH3

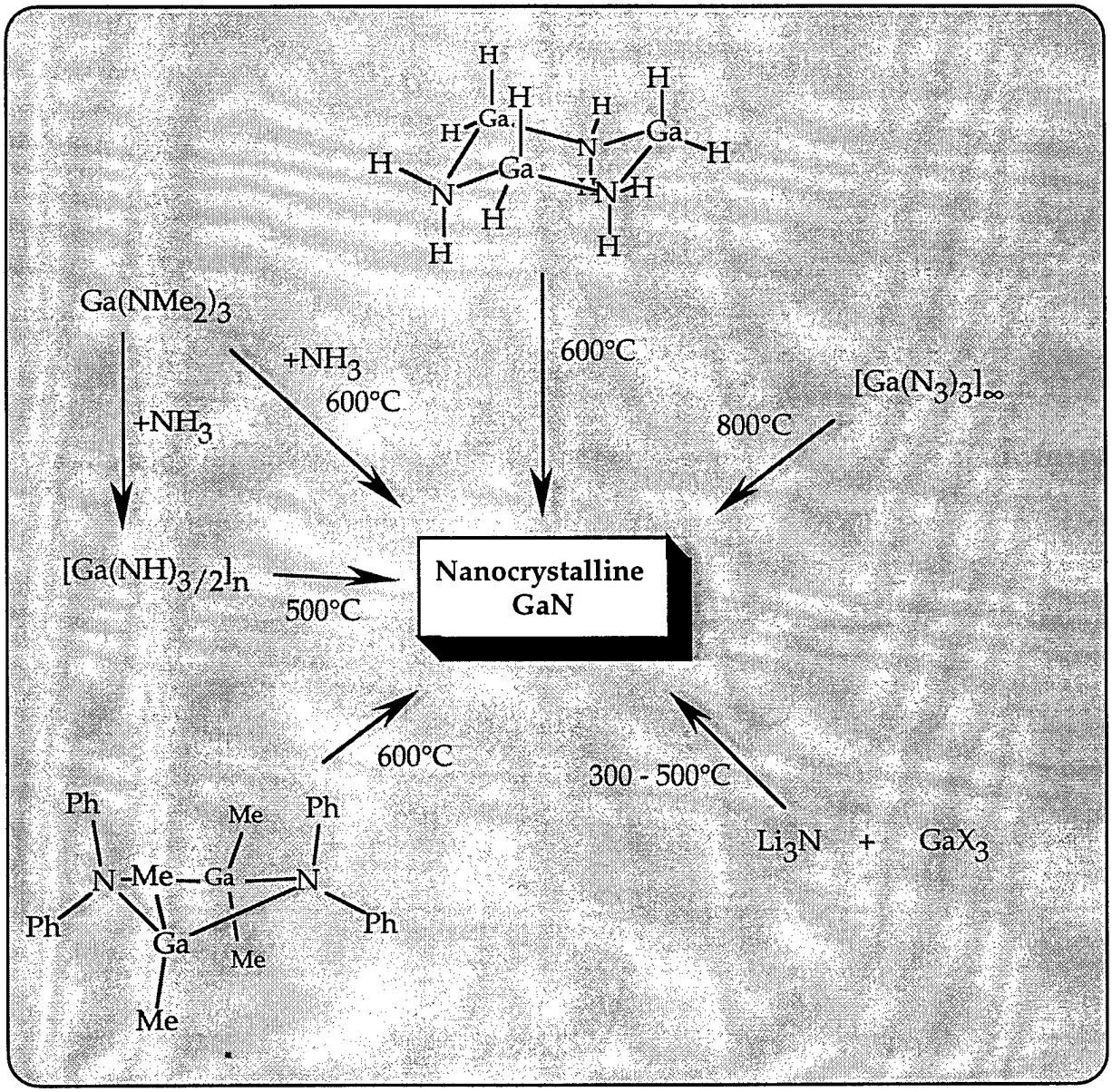
Ga(NMe2)3
+NH3
+NH3
600°C
600°C
[Ga(N3)3]∞
800°C
[Ga(NH)3/2]n
500°C
Nanocrystalline GaN
600°C
300 - 500°C
Li3N + GaX3

TECHNICAL REPORTS DISTRIBUTION LIST

ORGANOMETALLIC CHEMISTRY FOR ELECTRONIC & OPTICAL MATERIALS

Dr. Harold E. Guard
Code 1113
Chemistry Division, 331
Office of Naval Research
800 N. Quincy Street
Arlington, VA 22217-5660

Defense Technical Information
Center (DTIC)
Ft. Belvoir Headquarters Complex
8725 John J. Kingman Road
STE 0944
Ft. Belvoir, VA 22060

Dr. James S. Murday
Chemistry Division, Code 6100
Naval Research Laboratory
Washington, DC 20375-5320

Dr. John Fischer, Director
Chemistry Division, C0235
Naval Naval Air Weapons Center
Weapons Division
China Lake, CA 93555-6001

Dr. Richard W. Drisko
Naval Facilities & Engineering
Service Center
Code L52
Port Hueneme, CA 93043

Dr. Eugene C. Fischer
Code 2840
Naval Surface Warfare Center
Carderock Division Detachment
Annapolis, MD 21402-1198

Dr. Bernard E. Douda
Crane Division
Naval Surface Warfare Center
Crane, IN 47522-5000

Dr. Peter Seligman
Naval Command, Control and
Ocean Surveillance Center
RDT&E Division
San Diego, CA 93152-5000